Performance Enhancement of Fluidic Diode for a Wave Energy System through Genetic Algorithm

Emeel Kerikous [a,b] , Doddamani Hithaish [c], Abdus Samad [c] , Stefan Hoerner [a] , Dominique Thévenin [a]
[a] Lab of Fluid Dynamics & Technical Flows, Univ. of Magdeburg "Otto von Guericke",39106, Magdeburg, Germany
[b] Mechanical Power Engineering Department, Faculty of Engineering-Mattaria, Helwan University, 11718 Cairo, Egypt
[c] Wave Energy and Fluids Engineering Laboratory, Department of Ocean Engineering, Indian Institute of Technology Madras, Chennai-600036, India.

Abstract—**The oscillating water column (OWC) is a wave energy converter that utilizes sea wave motion to generate pneumatic power. However, its efficiency is hindered by poor flow blockage. To address this issue, researchers propose using a fluidic diode (FD) to enhance flow blockage. The FD's performance is evaluated based on its diodicity, which measures pressure drop in forward and reverse flows. Increased resistance in reverse flow indicates improved flow blockage, while lower resistance in forward flow reduces power loss at the turbine entry. The study employs numerical simulations with ANSYS-Fluent 16.1, solving three-dimensional unsteady Reynolds-Averaged Navier Stokes equations to analyze flow behavior within the FD. Five geometric parameters of the FD are varied to determine the optimal shape, which minimizes pressure drop in the forward direction and maximizes it in reverse. Using a genetic algorithm, the researchers achieve a 12% performance improvement compared to the base model. The article provides detailed fluid flow analysis and performance evaluation for both the base and optimum FD models.**

Keywords—**Air turbine, Fluidic diode, Optimisation, Oscillating water column, Wave energy.**

I. Introduction

Countries are reducing their reliance on fossil fuels for their energy needs as these sources are exhausting and negatively impact the environment. Hence, attention is shifted towards renewable energy, as these sources are non-exhausting and leave a small environmental footprint. Ocean energy is one of the renewable energy sources which is predictable and not affected by seasonal variation. Among the various concepts to harness ocean energy, an oscillating water column (OWC) device is popular due to its simple construction and operation. Figure 1 shows the schematic of OWC, which has a submerged water column, air chamber, and duct. As the wave reaches OWC, the water level in the water column rises, pushing air out.

Similarly, a receding wave lowers the water level and draws air. This action of OWC results in bi-directional pneumatic energy. A power take-off device, commonly an air turbine, converts this pneumatic energy into mechanical work.

The unidirectional turbine (UT) is similar to a conventional steam turbine, allowing it to extract power only for a particular airflow direction. Hence, it requires rectification to operate in oscillatory flow, which can be performed using a pair of mechanical valves. These valves pose a severe reliability issue because of their size and poor response time [1], [2].

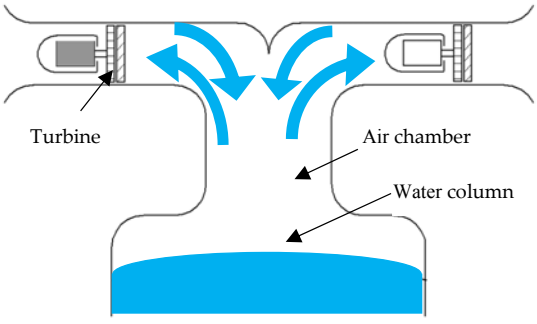

Fig. 1. Schematic of an OWC with UTs (turbine-duo) [3]

©2023 European Wave and Tidal Energy Conference. This paper has been subjected to single-blind peer review.

E.Kerikous, S.Hoerner, D.Thévenin are from Lab of Fluid Dynamics & Technical Flows, Univ. of Magdeburg "Otto von Guericke",39106, Magdeburg, Germany (e-mail: emeel.kerikous@ovgu.de , stefan.hoerner@ovgu.de, dominique.thevenin@ovgu.de).

D. Hithaish and A. Samad are with Wave Energy and Fluids Engineering Laboratory, Department of Ocean Engineering, Indian Institute of Technology Madras, Chennai-600036, India. (e-mail hithaishdoddamani@gmail.com, samad@iitm.ac.in)

Digital Object Identifier: https://doi.org/10.36688/ewtec-2023-182

a power extractor. In contrast, the other work as a flow blocker and this operation reverse itself, corresponding to wave motion. However, this is inefficient due to inadequate flow blockage [4]–[6]. A fluidic diode (FD) can be employed with a turbine duo to enhance the flow blockage [7]–[9]. It provides variable resistance to the flow depending on flow direction. Such FD are already used in microfluidic, nuclear applications, and pipes to prevent flow reversal [10].

Figure 2 shows the working of a simple nozzle-type FD [10]. In the forward direction, fluid leaves the nozzle smoothly with low resistance. In reverse, the same geometry acts as a diffuser offering higher resistance to the incoming flow. Its performance is given by diodicity (Ψ) (Eq. 1).

$$Diodicity\ (\Psi) = \frac{\Delta P\ (2-1)}{\Delta P\ (1-2)} \qquad (1)$$

Figure 3 shows some of the FD models found in the literature. Unlike other fluidic components, FD shapes are not standardised. Hence, a high potential for efficiency improvements using an optimized FD model with a specific design for wave energy systems can be hypothesized.

This article presents the numerical optimisation of a FD. The fluid flow and performance analysis of both the base and an optimised model are discussed.

II. Fluidic Diode Model

The present study considers an FD proposed for wave energy applications (Fig. 4) for optimisation [9]. The design is built on toroidal cup surrounding a bluff body (BD) with the shape of a half-crested moon, which is followed by a nozzle. The BD offers a smooth flow in the forward direction, where fluid flows over it and exits the diode. Whereas in reverse, due to the shape of the diode, the fluid experiences a higher resistance than forward.

III. Numerical Methodology

Figure 5 shows the three-dimensional computational domain considered for the study. The model consists of diode and duct. Since the geometry is symmetrical along the axis, only a sector of 45° is considered.

The computational domain was discretised into unstructured tetrahedral cells using the ANSYS ICEM CFD 19.1. Ten prism layers with 0.0304 mm initial height and an exponential growth rate of 1.15 are created on walls boundaries. Figure 5 shows the spatial discretised model; higher-density mesh elements are provided in the critical areas of the geometry.

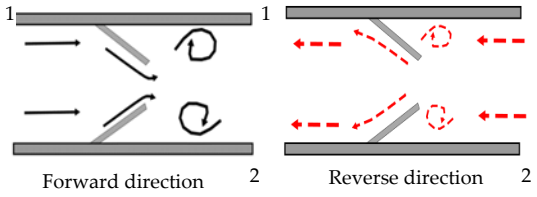

Fig. 2. Working principle of nozzle type diode [10]

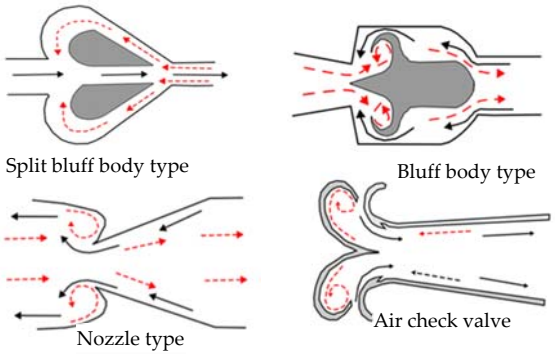

Fig. 3 Various FD models found in the literature [11]–[14]

A grid convergence index (GCI) study was employed to obtain the optimum number of mesh elements for the study [15]. It is a statistical method, requires three different mesh, with increasing refinement levels, starting from coarse (0.49 million N_3) to medium (1.39 million N_2) and finest mesh (3.88 million N_1). Parameters of interest for these grids are tracked and compared. Using the mathematical relationship, GCI was calculated, and its values are less than 1% for the successive grids. Hence numerical results will not change with subsequent refinement level for the spatial discretization which had been reached for mesh N_2. In consequence further numerical validation is performed using the medium grid (N_2). After the simulations, the maximum value of $y+$ were 0.62 and 0.92 in both directions, which are in the acceptable range.

In the forward direction, a constant flow rate was imposed on the inlet, and the outlet is opened to the atmosphere; these settings get reversed for the other direction. The pressure changes across the diode were measured for different flow rates.

The numerical investigation is performed using commercial computational fluid dynamic software ANSYS-Fluent 16.1. Table 1 provides the problem setup. Second-order upwind schemes were used to discretise convective terms.

Table 1. Numerical Model Setup

Parameter	Description
Analysis type	Unsteady
Discretisation scheme	Unstructured/Tetrahedral
Fluid	Incompressible air
Mach number (Max)	0.061
Residual convergence value	1×10^{-4}
Mass imbalance	0.001%
No. of inner iterations (Max)	3000

IV. Optimisation Methodology

The performance of FD is given by the diodicity, which is a ratio of the pressure drop in reverse to forward direction. Improving the resistance in the reverse direction can improve the overall performance of the FD. However, to use with a turbine duo, the resistance in the forward direction should be minimised to avoid any power loss at the entry of the turbine. Therefore, the above two contradicting objectives, i.e., 1) increasing the pressure drop of the FD in the reverse direction and 2) reducing the same in the forward direction, were used simultaneously as objectives for the present study. Euler number (Eu) (Eq. 2) represents the objective function, this non-dimensional number that provides the relationship in between pressure drop and velocity for a given direction.

$$\mathrm{Eu}\ (\xi)_{f/r} = \frac{\nabla P_{f/r}}{0.5 \times \rho \times u_{f/r}^2} \qquad (2)$$

The resistance experienced by the fluid flowing through the FD can be altered by changing its geometrical shape. Consider the shape of the base model (Fig. 4), constituted by the bluff body (BD) (constructed from R_{1B}, R_{2B}), toroidal section (R_{To}), and nozzle section (L_N, β). These sections offer resistance to the flow based on their shape. Hence, altering their shape affects the fluid flow characteristics and pressure drop in both directions. Variables responsible for the shape of the diode (R_{1B}, R_{2B}, R_{To}, L_N, β) are considered as design variables. Table 2 provides the upper and lower limit set for the geometric model.

Different geometrical configurations obtained by varying the design limits are numerically investigated, as discussed in the methodology section. The pressure drop for both flow directions is measured. This data is stored in an output file and fed to OPAL++, which decides the new geometries for subsequent generation and constructs the Pareto optimum front. The Otto von Guericke University Magdeburg, Germany, developed the OPAL++ optmisation software. It was used in several similar optimisation problems in the past [16]–[19]. Figure 6 shows the schematic of the optimisation framework.

V. Results and Discussion

A. Numerical validation

Figure 7 shows the comparison of the numerical results with the experiment. The right side of the graph indicates the forward flow, while the left side (negative flow) indicates the reverse flow. As the flow rate increases, the pressure drop increases in both directions. However, the increment in pressure drop in the reverse flow is higher than in the forward. The numerical model (activating the k-ω SST turbulent closure model) can predict correctly the experimental results in both flow directions.

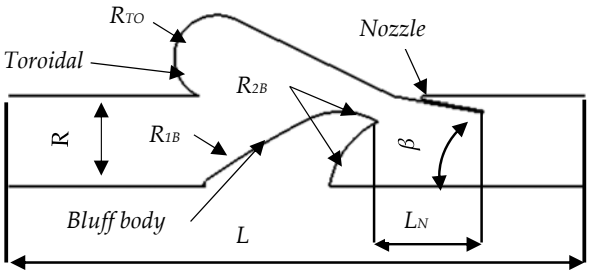

Fig. 4. Bluff body type fluidic diode [9]

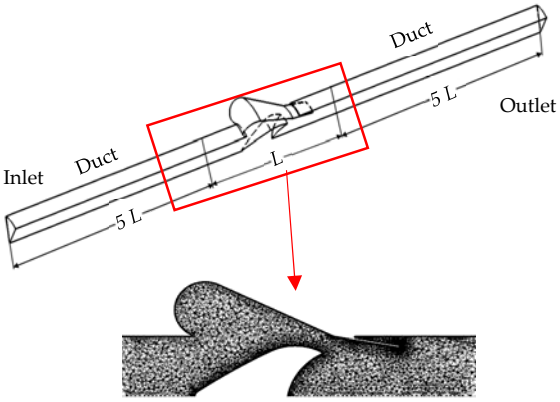

Fig. 5. Computational domain of the FD

TABLE 2. Bounds of the Design Variables Considered for the Study

	Upper bound	Base model	Lower bound
R_{1B}	5.079	4.833	4.587
R_{2B}	0.629	0.416	0.173
R_{To}	0.847	0.476	0.429
L_N	0.949	0.500	0.304
β	20.0	10.0	5.0

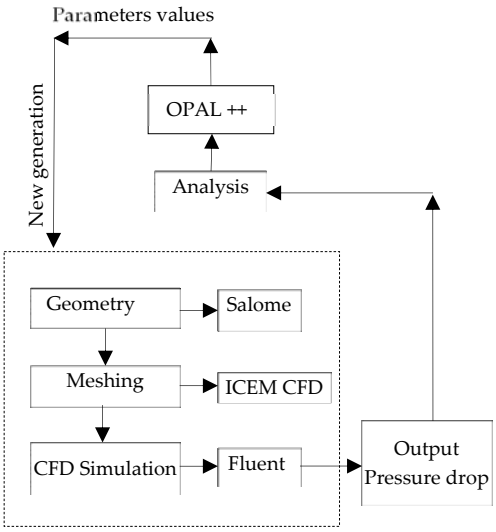

Fig. 6. OPAL++ framework

B. *Optimisation results*

The optimal solutions obtained for different configurations can be excellent in one objective but poor in another. Such solutions are said to be non-dominated solutions, and the curve joining such solutions is called the Pareto front. Figure 8 presents the Pareto-optimal solutions after five generations, each involving 50 individuals, as obtained from OPAL++. The *x*-axis represents Eu in the forward direction, and the *y*-axis represents the same in reverse direction. It can be observed that the values of the two objectives increase simultaneously for all configurations.

The diode proposed for wave energy should have a minimal pressure drop across the turbine so that it does not hamper its performance. At the same time, it should have maximal flow blockage efficiency (diodicity) to block the reverse flow effectively. An optimum design should have a lesser pressure drop in the forward direction than the base model. At the same time, it should show a higher pressure drop in the reverse direction, as shown in Figure 8.

The retained optimum design has 12% higher diodicity than the base model, and its variation of pressure drop for the flow rate is shown in Figure 9. Similar to the base model, here, also pressure drop increases with an increase in flow rate. However, it has a higher pressure drop in the reverse direction than the base model for the whole range of flow rates considered. The pressure drop varies linearly with the flow rate because, at a higher flow rate, drag friction contributes to the overall pressure drop due to the complex shape of the FD.

As the performance of the diode varies linearly with the flow rate, a single flow rate was considered instead of considering the variation of fluid properties for different flow rates. To analyse the flow physics inside the optimum and base model, the streamline distribution and pressure were obtained at the mid-portion of the diode for 0.27 m³/s.

C. *Streamline distributions*

1) *Forward direction*

Figure 10 illustrates the streamline contours along the flow path as it approaches the FD. Upon reaching the FD, some fluid streams adhere to the duct wall and leak into the cup section before encountering the bluff body. The leaked fluid attempts to blend with the main flow but is impeded by higher flow velocity surrounding the bluff body, forming a cavity vortex. The physical dimension of the cup limits its size.

As the flow encounters the FD, it interacts with the obstruction posed by BD. When the fluid comes in contact with the BD profile, its velocity becomes zero due to the no-slip condition. The fluid tends to conform to the shape of the BD, causing a velocity to drop along its surface. However, the flow velocity increases in the smaller area of the cup.

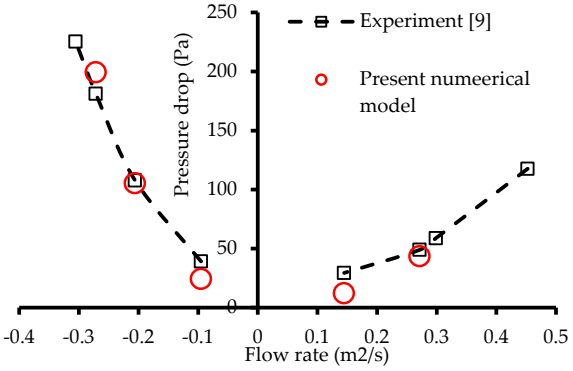

Fig. 7. Numerical validation with experimental results

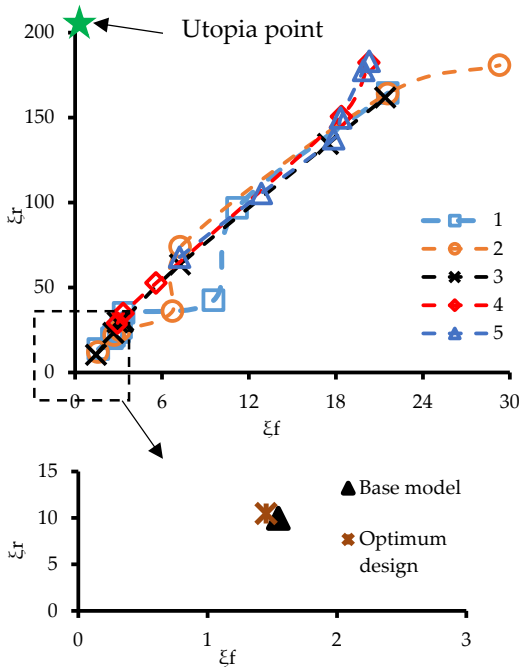

Fig. 8. Numerical validation compared to experimental results

TABLE 3. COMPARISON BETWEEN THE BASE AND OPTIMISED MODEL

		Base model	Optimum model
Geometric parameters	R_{1B}	4.883	4.679
	R_{2B}	0.416	0.364
	R_{TO}	0.476	0.350
	L_N	0.5	0.496
	β	10	11
Objectives	ξ_f	1.460	1.451
	ξ_r	9.490	10.471
Performance parameter	Ψ	6.435	7.212

This differential velocity and the abrupt change in the BD profile create an adverse pressure gradient, causing the fluid to detach at the ends. The detached flow then attaches to the corner of the BD, resulting in a wake region.

When the fluid exits the nozzle, the flow path experiences sudden expansion. Due to the adverse pressure gradient and momentum difference caused by

the nozzle steepness, the fluid separates after the nozzle walls. The separated fluid attaches to the duct wall after a certain distance (reattachment length), which is affected by the shape of the nozzle section.

2) Reverse direction

For the reverse flow (Fig. 10), the fluid coming from the nozzle encounters obstruction and initiates a backflow along the nozzle walls. However, its growth is limited by the angle between the cup and the nozzle wall. Since both models have similar nozzle lengths, the vortex strength remains identical.

As the fluid progresses beyond the nozzle section, it encounters the convex shape of the BD (formed by R_{2B}). This resembles a curved vane, causing the incoming flow to deflect and obstruct. The fluid gains velocity within the smaller area of the BD and cup section. However, the accelerated fluid that attempts to draw the vortex along the flow on the BD is stopped by the surrounding fluid in the toroidal section.

The curved profile of the cup forces the vortex to attach to the BD's surface. Consequently, the outer layer of the fluid exhibits greater circular momentum. As a result, the fluid attempting to exit the toroidal cup section cannot follow the orderly motion at the duct. This results in a recirculation zone at the exit of the cup section. The intensity of the vortex is higher for the optimum model than for the base model.

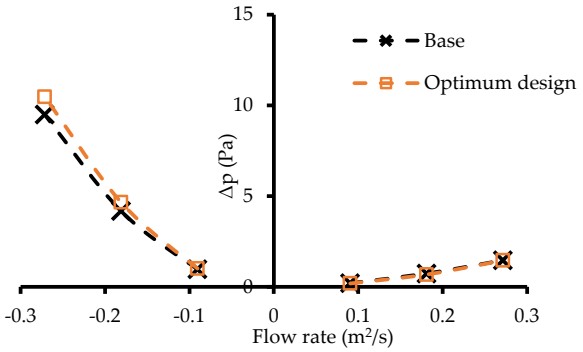

Fig. 9. Comparison of base and optimal design

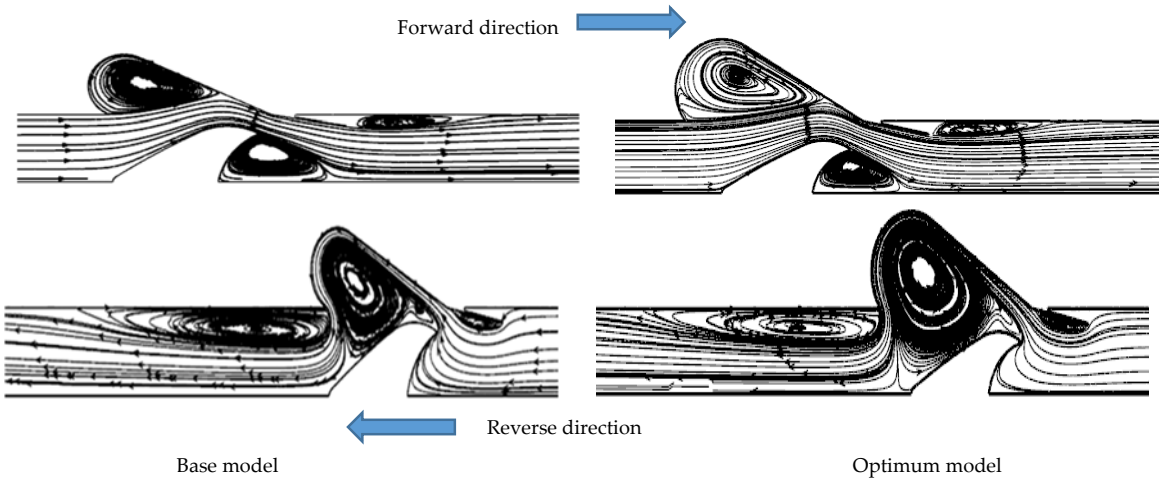

Fig. 10. Numerical validation with experimental results

D. Pressure distribution

Figure 11 shows the static pressure contours of the diode along the length. For the forward flow, the presence of the BD generates a stagnation zone, leading to the deceleration of the fluid resulting in higher pressure. The flow velocity increases as the available flow area decreases around the BD. When fluid exits the diode viva nozzle, it undergoes a conversion of pressure energy to kinetic energy to preserve the fluid's total energy. Consequently, a lower pressure distribution is observed at the end of the nozzle. The behaviour is consistent across all the models in the forward direction.

In reverse flow, the fluid coming through the nozzle undergoes diffusion, offering higher resistance to fluid entry. As a result, a higher pressure drop occurs in this section. Subsequently, the fluid stream exiting through the toroidal and BD section experiences higher resistance.

The geometry of the FD in the forward direction features a streamlined BD, resulting in a reduced surface area opposing the flow. Consequently, the fluid flow experiences reduced skin friction drag in the forward direction. Conversely, in the reverse direction, the geometry is exposed to a larger surface area to the flow due to the convex shape of the BD, leading to increased form and skin friction drag. These characteristics are evident from the pressure contours observed in both flow direction

Fluid flowing through the optimum model experiences lesser resistance around the BD in the forward direction as it has approximately a 30% broader gap between the cup and the BD than the base model.

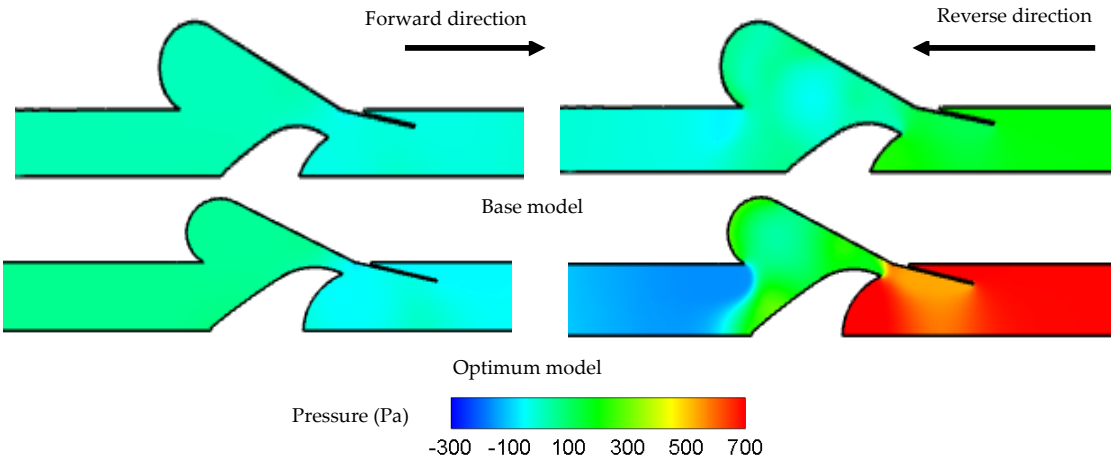

Fig. 11. Numerical validation with experimental results

VI. Conclusion

In this study, the shape of the fluidic diode (FD) utilized for wave energy application was optimized using the non-dominated sorting genetic algorithm-II, a genetic algorithm. The primary objectives were to minimize the pressure drop in the forward direction and maximize it in the reverse direction.

The optimisation process was conducted using OPAL++. The optimal design exhibited superior performance compared to the reference model, achieving a 12% higher diodicity at a flow rate of 0.27m3/s. Moreover, the fluid experienced reduced resistance in the forward direction due to a approximately 30% wider gap between the cup and the BD compared to the reference model.

ACKNOWLEDGEMENT

Doddamani Hithaish would like to thank Indo-German Center for Sustainability (IGCS) for providing a scholarship to undertake this project.

Abbreviations

BD	Bluff body
CFD	Computational fluid dynamics
Eu	Euler number
FD	Fluidic diode
GCI	Grid convergence index
OWC	Oscillating water column
UT	Unidirectional turbine

Symbols

β	Nozzle angle (degree)
ΔP	Pressure drop (Pa)
ξ	Euler number
ρ	Density (kg/m^3)
R	Normalised radius
L	Length (m)
u	Free stream velocity (m/s)
ω	Angular speed (rad/s)
k	Turbulent kinetic energy (m^2/s^2)
Ψ	Diodicity

Subscripts

B	Bluff body
N	Nozzle
f	Forward
r	Reverse
To	Toroidal

REFERENCE

[1] T. K. Das, P. Halder, and A. Samad, “Optimal design of air turbines for oscillating water column wave energy systems: a review,” *Int. J. Ocean Clim. Syst.*, vol. 8, no. 1, pp. 37–49, 2017.

[2] A. F. O. Falcão and J. C. C. Henriques, “Oscillating-water-column wave energy converters and air turbines: a review,” *Renew. Energy*, vol. 85, no. 1, pp. 1391–1424, 2016.

[3] T. V. Heath, “A review of oscillating water columns,” *Philos. Trans. R. a scoiety*, vol. 370, pp. 235–245, 2012.

[4] V. Jayashankar *et al.*, “A twin unidirectional impulse turbine topology for OWC based wave energy plants,” *Renew. Energy*, vol. 34, no. 3, pp. 692–698, 2009.

[5] K. Mala *et al.*, “A twin unidirectional impulse turbine topology for OWC based wave energy plants - experimental validation and scaling,” *Renew. Energy*, vol. 36, no. 1, pp. 307–314, 2011.

[6] M. Takao, A. Takami, S. Okuhara, and T. Setoguchi, “A twin unidirectional impulse turbine for wave energy conversion,” *J. Therm. Sci.*, vol. 20, no. 5, pp. 394–397, 2011.

[7] P. V. Dudhgaonkar *et al.*, “Fluidic components for oscillating water column based wave energy plants,” in *ASME-JSME-KSME 2011 Joint Fluids Engineering Conference, 24-29 July, 2011.*, 2011.

[8] S. Okuhara, H. Sato, M. Takao, and T. Setoguchi, “Wave energy conversion : effect of fluidic diode geometry on the performance,” *Open J. Fluid Dyn.*, vol. 4, pp. 433–439, 2014.

[9] S. Okuhara, A. M. M. Ashraful, M. Takao, and Y. Kinoue, “Performance of fluidic diode for a twin unidirectional impulse turbine,” in *Earth and Environmental Science 16-21 September,2018.Kyoto, Japan*, 2019, vol. 240, no. 5.

[10] S. K. Thomas and T. M. Muruganandam, “A review of

acoustic compressors and pumps from fluidics perspective," *Sensors Actuators A. Phys.*, vol. 283, no. 11, pp. 42–53, 2018.

[11] H. G. Tucker, "Fluidic diode," US3604442, 1971.

[12] M. E. Suchezky and J. B. Drobnis, "Valvular conduit exhaust Manifold," US2019/0162104A1, 2019.

[13] C. C. K. Kwok, "Vortex vent diode," US3461897, 1969.

[14] L. E. Torvald, "Aerodynamic check valve," US2727535, 1995.

[15] I. B. Celik, U. Ghia, P. J. Roache, C. J. Freitas, H. Coleman, and P. E. Raad, "Procedure for estimation and reporting of uncertainty due to discretization in CFD applications," *J. Fluids Eng. Trans. ASME*, vol. 130, no. 7, pp. 1–14, 2008.

[16] E. Kerikous and D. Thévenin, "Optimal shape and position of a thick deflector plate in front of a hydraulic Savonius turbine," *Energy*, vol. 189, 2019.

[17] E. Kerikous and D. Thévenin, "Optimal shape of thick blades for a hydraulic Savonius turbine," *Renew. Energy*, vol. 134, no. November, pp. 629–638, 2019.

[18] L. Daróczy, G. Janiga, and D. Thévenin, "Systematic analysis of the heat exchanger arrangement problem using multi-objective genetic optimization," *Energy*, vol. 65, pp. 364–373, 2014.

[19] T. K. Das, E. Kerikous, N. Venkatesan, G. Janiga, D. Thevenin, and A. Samad, "Performance improvement of a Wells turbine through an automated optimization technique," *Energy Convers. Manag. X*, vol. 16, no. March, 2022.